Mechanical Design of Ultra-Thin White-Topping with High Strength Concrete Panel

<Tatsuo Nishizawa[1], Hiroyuki Obata[2], and Iwao Sasaki[3]>

Abstract

An ultra-thin white-topping structure with high strength concrete panel (HSCWT) was developed. In the structure, 30 mm thick concrete panels, which are produced from steel fiber reinforced concrete with a flexural strength of 20 MPa, are placed on an existing asphalt pavement and the interface between the panels and the asphalt pavement is grouted to bond them. Test pavements of HSC-WT were constructed on an accelerated loading facility and were subject to moving axle loads. After one hundred fifty thousand axles passed over the pavements, although small gaps developed between HSC panels and grout near joints, any severe cracks didn't develop. Improved textures on the bottom face of panel were found very effective to bond the panel and grout. Although simulation of the loading test with dynamic 3DFEM fairly well represented the strain time histories generated by the travelling axle load, visco-elastic properties of asphalt layer could not clearly identified. Stress analysis with assumed visco-elastic parameters revealed that the stresses in the panel due to axle load are much less than the strength of the HSC panel, if the panel and the grout is fully bonded at the interface. Based on the results, a mechanical design procedure for HSCWT is developed. In the procedure, tensile strains in the underlying asphalt layer are calculated with 3DFEM and fatigue damage of the asphalt layer is estimated from the tensile strains using fatigue curve of asphalt mixture. It was found that not only viscosity of asphalt layer but also vehicle speed significantly affects fatigue life of asphalt layer.

[1] Professor, Ishikawa National College of Technology. Address: Tsubata, Ishikawa 929-0392 JAPAN
E-mail: nishi@ishikawa-nct.ac.jp
[2] Taiheiyo Cement Corporation. Address: 2-4-2 Taisaku, Sakura, Chiba 285-8655 JAPAN
E-mail: Hiroyuki_Obata@taiheiyo-cement.co.jp
[3] Principal Researcher, Public Work Research Institute. Address: 1-6 Nanbara Tsukuba, Ibaragi 305-8516 JAPAN
E-mail: isasaki@pwri.go.jp

Introduction

In this study, an ultra-thin white-topping structure with an ultra high strength fiber reinforced concrete whitetopping (HSCWT), has been developed. In this method, 1.0 m by 1.7 m panels with a thickness of 30 mm. The panels are prefabricated in a factory under carefully controlled curing conditions and are placed over an existing asphalt pavement. The flexural strength of the HSC panels is more than 20 MPa, which is much higher than normal concrete slabs (Uzawa, T. et al., 2002). The panels are bonded with the asphalt layer by grouting the gap between them.

For the rational structural design of the HSCWT, mechanical behavior of the structure should be thoroughly understood. Although the HSC panels have high flexural strength, stresses in the panels due to traffic loads are expected to be high and strongly dependent upon the stiffness and thickness of the underlying asphalt layer. Furthermore, since the asphalt layer is much thicker than the panels, its visco-elastic nature should be taken into account.

This paper investigates the mechanical behavior of an HSCWT structure due to traffic load based on experimental examinations on full-scale test pavements constructed in an accelerated pavement testing (APT) facility and a dynamic 3DFEM analysis. Effects of visco-elastic nature of the underlying asphalt layer and loading rate on stresses in the HSC panels and strains in the asphalt layer are examined.

Based on the results, a mechanical design procedure for HSC-WT is developed. In the procedure, tensile stresses in HSC panels and tensile strains in underlying asphalt layer are calculated with 3DFEM and possibilities of fatigue cracks in the panels and the asphalt layer are examined. The main feature of this procedure is the consideration of fatigue damage for both HSC panel and underlying asphalt layer.

Loading Tests

In order to investigate long term performance of HSCWT under traffic loadings, test pavements were constructed in an APT facility (Sasaki et al. 2004), which is capable of repeatedly applying a large vehicle load traveling over the pavements. The loading vehicle has the same features of commercially available trucks in Japan with a tandem rear axle load (front axle: 109 kN and rear axle: 100 kN). Two sets of loading test were conducted. The first loading test was conducted in the late summer, 2002 (Nishizawa et al. 2005) and the second one was conducted in the late winter, 2006.

In the first loading test, very small surface cracks were observed in the HSC panels after 200,000 load passes. From core observation, it was found that interface between the panel and grout was unbonded in some areas because of special textured bottom surface of the panel. Based on the finding, the second loading test was conducted to examine effectiveness of improved bonding methods. In the following sections, overview and results of the second loading tests will be presented.

Overview

In the second loading test, HSCWT test pavements, as shown in Figure 1, were constructed and were subjected to 150,000 axle load passes. Since the bonding method for the interface between the panels and grout in the first loading test had not succeeded, the bottom surface texture of the panels was modified. Two types of texture were adopted, as shown in Figure 2. The first one was the Stone type, in which half portion of each stone aggregate is stuck out on the surface. The second one was the Coin type, which looks like that small coins are attached on the surface. The grouting material was basically Portland cement mixture. During the repeated loading, surface conditions were observed and bonding condition was monitored with hammering test. Furthermore, strains at the top and bottom of the panel and strain at the top of the asphalt layer were measured. The traveling speed of the vehicle was varied from 5 km/h to 15 km/h in the strain measurement to investigate the effect of loading rate on the strains.

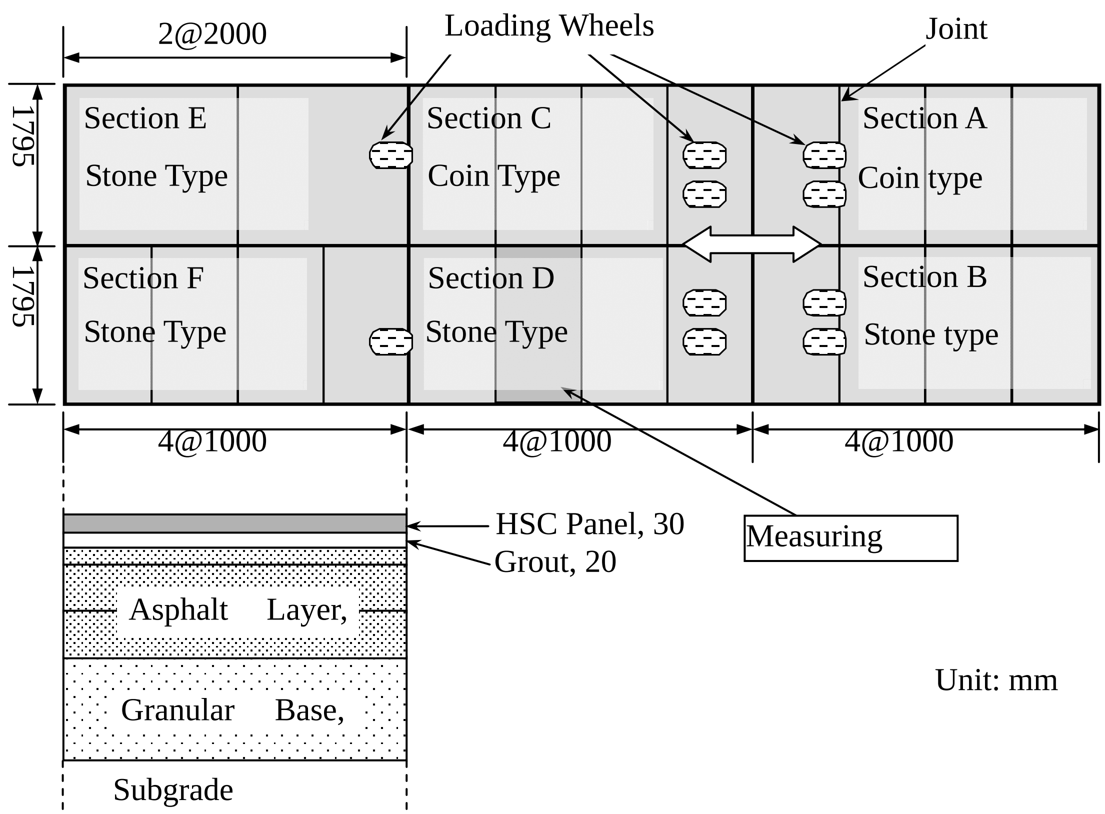

Figure 1. Pavement Sections of HSC-WT in the Second Loading Test.

(a) Stone Type

(b) Coin Type

Figure 2. Modified Textures on the Bottom Face of Panels in the Second Loading Test.

Results

In the second loading test, no surface crack appeared after 150,000 wheel load had passed. Although some unbonded areas were detected near the joints as shown in Figure 3, the amount of the area was much less than those in the first loading test. This result suggests the effectiveness of the modified types of textures on the bottom face of the panels. On the whole, the performance of the HSCWT was very satisfactory in this test.

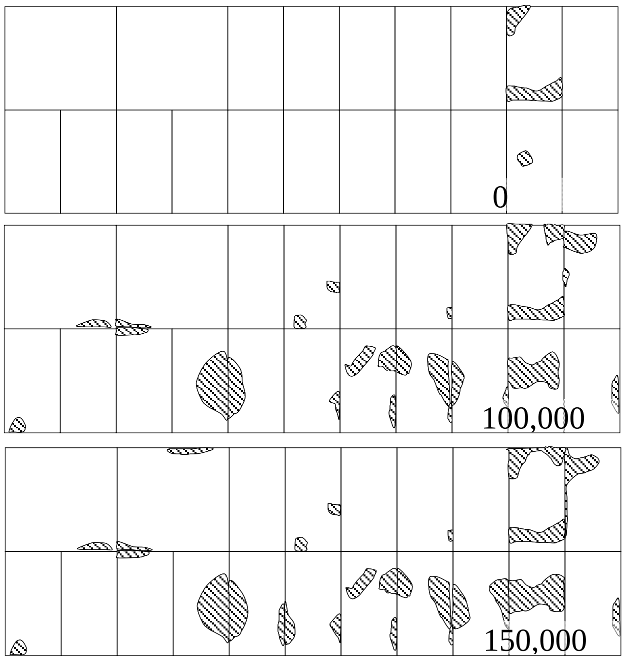

Figure 3. Unbonded Areas Judged from Hammering Sound in the Second Loading Test.

FEM Analysis of Loading Tests

Structural Model

In order to analytically investigate the mechanical behavior of HSCWT, a 3DEFM program, Pave3D, was employed in this study (Nishizawa et al. 2003). In this program, joint is modeled with an interface element, in which load transfer at the joint is represented by three linear elastic springs. Similarly, the interface element is inserted between the concrete slab and the grout layer. If the concrete slab is bonded with the grout layer, all spring constants are set at a very high value. On the other hand, if the concrete slab is unbonded with the grout layer and there is a slip between them, very low values are given for the springs parallel to the interface.

Figure 4 shows a 3DFEM mesh for the analysis of the test pavement. Considering the symmetric structural conditions, only a half region of the pavement was meshed in the model. The 130 mm asphalt mixture layer and 100 mm asphalt stabilized layer were treated as a single 230 mm asphalt layer. The panels, grout and asphalt layer as well as a 200 mm thick granular base course and a 1000 mm thick subgrade were meshed with solid elements. The joints between the panels were assumed to have no load transfer ability. Rectangular uniform loads that had the same tire arrangements and load magnitudes as the APT loading vehicle were traveling in the longitudinal direction (x-direction) at a specified operating speed.

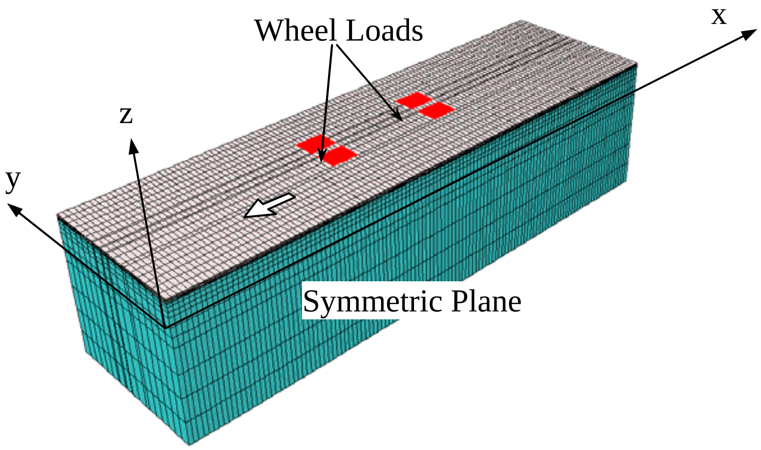

Figure 4. 3DFEM Model for Test Pavement

Input Parameters

Material properties of structural elements are summarized in Table 1. All materials except for the asphalt mixture were assumed to be linear elastic. Elastic properties of the HSC panels and grouting layer were obtained from laboratory tests and those of the base course and subgrade were determined from falling-weight deflectometer (FWD) deflections by a back-analysis program of BALM99 (Matsui et al. 2006).

Table 1. Material Properties

Material or Structural Element	Elastic Modulus (MPa)	Poisson's Ratio	Unit Mass (g/cm^3)
HSC Panel	30000	0.2	2.4
Cement Grout	1000	0.2	2.3
Granular Base Course	300	0.35	1.8
Subgrade	30	0.35	1.6

Burger Model was employed to describe the visco-elastic behavior of asphalt layer, as shown in Figure 5 (Huhtala et al. 1992). Three types of visco-elastic property of asphalt mixture were assumed as presented in Table 2. Two interface conditions between panel and grout were taken into account: rough and smooth. The rough interface is the case where panel and gout are completely bonded, while the smooth interface is the case where both are unbounded and there is a gap between them. The other interfaces in the pavement were assumed to be rough as summarized in Table 3.

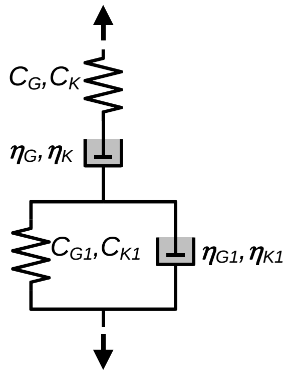

C_G = Shear Elastic Compliance of Maxwell Component,
C_G = Volume Elastic Compliance of Maxwell Component,
η_G = Shear Viscosity Modulus of Maxwell Component,
η_K = Shear Viscosity Modulus of Maxwell Component,
C_{G1} = Shear Elastic Compliance of Voigt Component,
C_{K1} = Volume Elastic Compliance of Voigt Component,
η_{G1} = Shear Viscosity Modulus of Voigt Component,
η_{K1} = Shear Viscosity Modulus of Voigt Component,

Figure 5. Burger Model for Asphalt Mixture

Table 2. Visco-elastic Properties of Asphalt Layer

Parameters	V-0	V-1	V-2
E [MPa]	7000	7000	7000
η_G η_{G1} [MPa*sec]	--	$5*10^4$	10^4
E_1 [MPa]	--	7000	7000
η_K, η_{K1} [MPa*sec]	--	10^8	10^8

Note: $C_G = 2(1+\mu)/E$, $C_{G1} = 2(1+\mu)/E_1$, μ is Poisson's ratio.

Table 3. Interface Properties

Interface	Condition	k_s [MN/m^3]	k_t [MN/m^3]	k_n [MN/m^3]
HSC Panels & Grouting	Rough	100000	100000	100000
	Smooth	10	10	100000
Grouting & Asphalt Layer, Asphalt & Base Course, Base Course & Subgrade	Rough	100000	100000	100000

k_s, k_t : Springs parallel to interface plane, k_n: Spring perpendicular to interface plane.

Computation results

Figure 6 shows comparisons between measured and computed strain time histories at the top and bottom of the panel and at the top of the asphalt layer. Since the bonding condition between the panel and grout was observed to be very good in the loading test, the rough interface condition between them was assumed in the simulation. At the top of the panel, as the axle load approaches, transverse strain, e_y, increases in negative and reaches a peak when the axle passes over the point. Longitudinal strain, e_x, on the other hand, increases in positive and reverses very quickly into a negative peak when the axle passes over the point. The effect of visco-elasticity appears on the peak strain: the peak value of strain becomes greater as the viscosity decreases from V-0 to V-2. At the bottom of the panel, values of the strains are much less than those at the top. The measured e_x are positive when the axle passes over, while the computed e_x is still negative. Similarly, at the top of asphalt layer, the measured e_x is positive while the computed one is negative. The measured strains are much less than the computed ones.

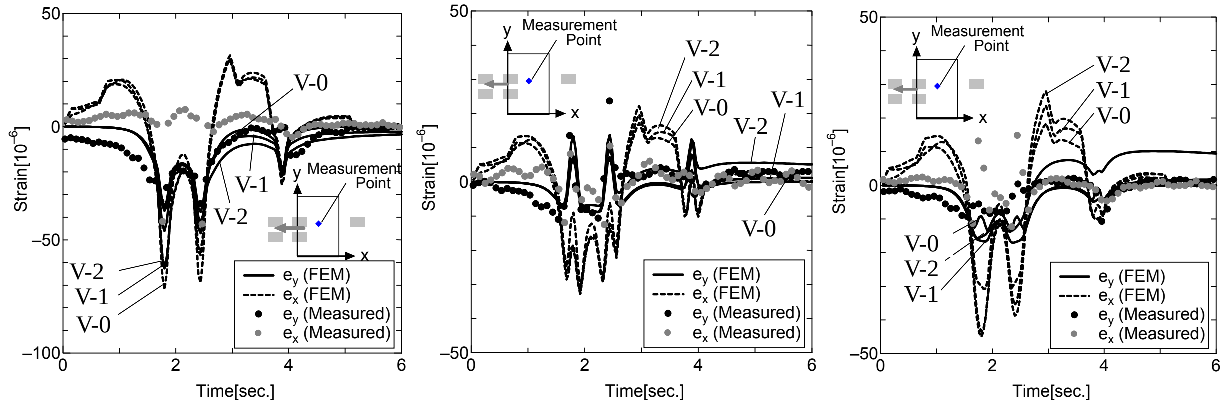

(a) Top of Panel (b) Bottom of Panel (c) Top of Asphalt Layer

Figure 6. Measured and Computed Strains in the Second Loading Test

Figure 7 shows the horizontal strain distribution throughout pavement depth at the panel center, when a rear axle load passes just over the point. In the panel, the measured strains are negative at the top, and positive at the bottom except for the computed e_x that is still negative at the bottom. Although the measured strains are less than the computed ones, the measured and computed strain distributions have similar tendency. In the asphalt layer, however, complete comparison is not possible, because the measuring point was only one and measured strains were very small, which probably contained relatively large errors.

Although perfectly good agreements between the measured and computed strains could not be obtained, it is assumed in this study that 3DFEM simulations with the material models of V-0 to V-2 are able to predict the mechanical behavior of entire pavement structure. It would be justified from the previous study, where very good agreement was obtained (Nishizawa, T. et al., 2005).

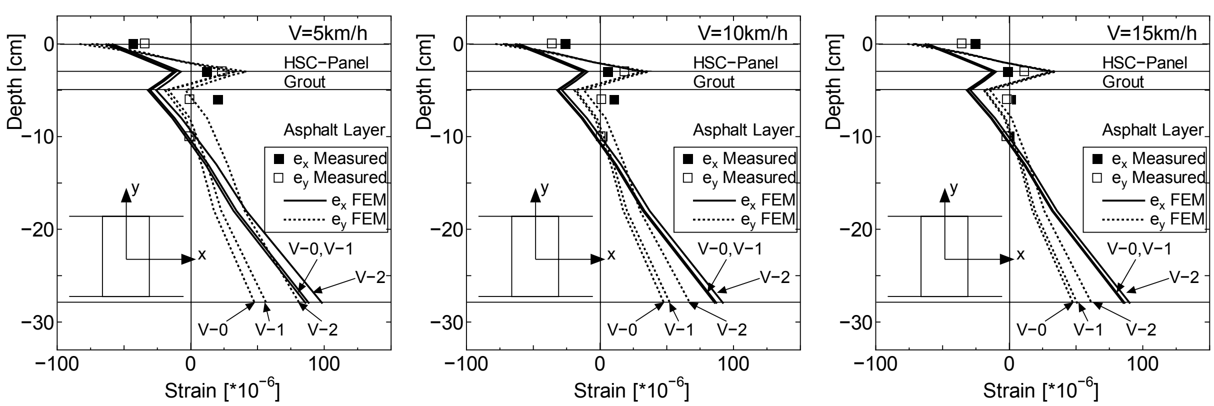

Figure 7. Strain Distributions throughout Pavement Depth

Structural Design of HSC-WT

Concept

In the structural design of HSCWT proposed in this study, fatigue cracking in both HSC panel and underlying asphalt layer are taken into account. In order to avoid the fatigue cracking during a design period, fatigue analysis should be performed using bending stress in HSC panel and tensile strains in asphalt layer and fatigue curves. In this section, bending stress in HSC panels and tensile strain will be discussed based on the 3DFEM analysis.

Stresses in HSC-Panel

Table 5 summarizes the maximum and minimum stresses generated in the HSC panel by the axle loads for each visco-elastic model at 5km/h speed. The interface condition between the panel and grout significantly affects on the stresses. Tensile S_x at the top of the panel in the rough interface is larger than that in the smooth interface that is the worst case, while S_x and S_y at the bottom in the smooth condition are larger than that in the rough condition. Therefore, cracks from the surface would more likely occur in the rough interface, while cracks from the bottom would occur in the smooth interface. Nevertheless, those values are much less than the strength of HSC panel of 20 MPa, if the full bonding and support exist. Therefore, it is concluded that the fatigue of the panel is not an issue in HSCWT.

Table 5. Stresses in HSC Panel Generated by Axle Load (MPa)

Visco-elastic Model			V-0	V-1		V-2	
Interface Condition			Rough	Rough	Smooth	Rough	Smooth
Top of Panel	S_x	Max.	0.92	0.89	0.21	0.90	0.18
		Min.	-2.71	-2.34	-1.07	-2.37	-1.12
	S_y	Max.	0.13	0.12	0.03	0.12	0.05
		Min.	-2.11	-1.73	-1.10	-1.87	-1.24
Bottom of Panel	S_x	Max.	0.54	0.62	0.93	0.72	0.97
		Min.	-0.97	-1.02	-0.20	-1.01	-0.14
	S_y	Max.	0.31	0.17	0.88	0.31	1.03
		Min.	-0.40	-0.43	-0.01	-0.37	0.00

S_x: Stress in x direction, S_y: Stress in y direction. +: Tensile stress, -: Compression stress

Strain in Asphalt Layer

If stresses in HSC-panel are much less than its strength and durability of the panel is ensured in terms of fatigue cracking, the critical failure mode might be fatigue cracking in underlying asphalt layer. In this section, durability of underlying asphalt layer will be examined by performing fatigue analysis for the asphalt layer using tensile strain at the bottom of the layer and fatigue curve of asphalt mixture.

In order to find the most critical point in the asphalt layer, strain distributions at the bottom of the asphalt layer were calculated as shown in Figure 8. Since the strain in the x direction, e_x, is greater than that in y direction, e_y, as can be seen in Figure 8, e_x will be discussed in the following. From these figures, it can be noticed that e_x is much greater when a wheel is located just over the joint than when the wheel is located between the joints. It is because the joint reduces the bending stiffness of the panel layer, resulting in large strains at the bottom of the asphalt layer.

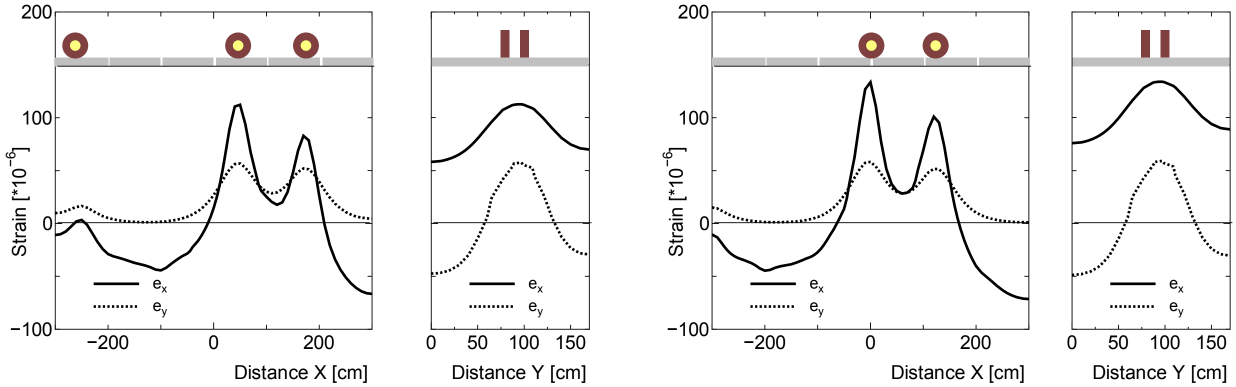

(a) Center Loading (b) Joint Loading

Figure 8. Strain Distribution at the bottom of asphalt layer (Vehicle Speed =5km/h, Material Model:V-0)

Figure 9 shows the effect of vehicle speed and viscosity of the asphalt layer on the magnitude of e_x just under the joint. When the vehicle speed is high and the viscosity is also high, e_x of the front wheel of the tandem axle is slightly greater than that of the rear wheel, because this vehicle happened to have a greater load on the front axle than that on the rear axle. However, when the vehicle speed is low and the viscosity is also low, e_x of the rear wheel is greater than that of the front wheel. It is because the e_x of the front wheel still remains when the rear wheel passes over the point because of the effect of viscosity. Therefore, if both axles have the same load, e_x of the rear axle may be larger than that of the front axle.

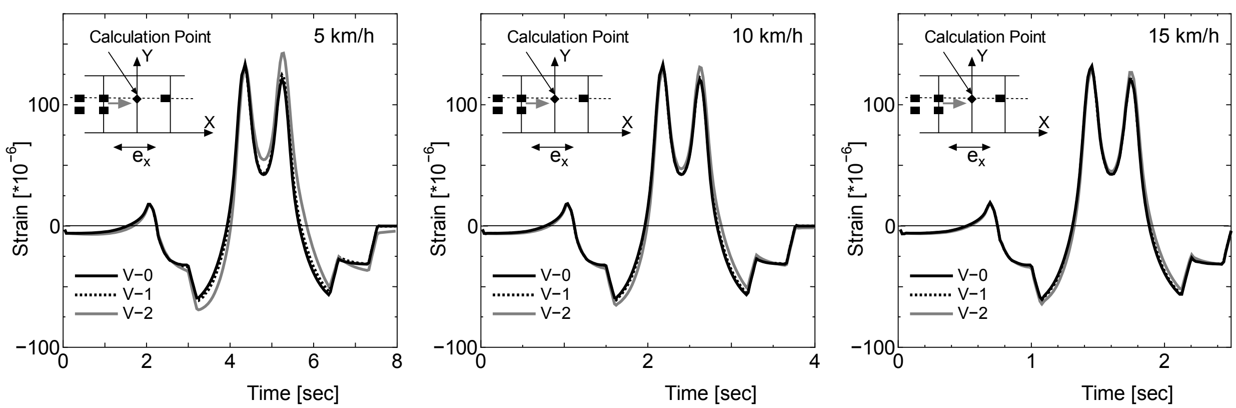

(a) Vehicle Speed = 5km/h (b) Vehicle Speed = 10km/h (c) Vehicle Speed = 15km/h

Figure 9. Strain Variation at the Bottom of Asphalt Layer

In this study, the fatigue life N_f was estimated from the following fatigue curve (Japan Road Association 2007):

$$N_f = 18.4C(6.617 \times 10^{-5} e_x^{-3.291} \times E_A^{-0.854}) \qquad (1)$$

where, N_f: number of load repetitions to failure, E_A: elastic modulus of asphalt (MPa), $C = 10^M$, $M = 4.84(V_b/(V_b+V_v)) - 0.69$, V_b: binder content in volume %, and V_v: void content in volume %. Assuming that E_A=7000 MPa, V_b=12.5% and V_v = 4%, fatigue life that is expressed as the number of repeated wheel loads of 49 kN, N_f, was estimated for each computed tensile strain, e_x, that is generated by 49 kN wheel load.

Table 6 summarizes e_x and N_f computed for each vehicle speed and material model. The tensile strain e_x increases as the viscosity of asphalt layer decreases from V-0 to V-2 and the vehicle speed decreases from 10km/h to 5 km/h. This increase of e_x results in the decrease of the fatigue life. Nevertheless, the least fatigue life in the HSCWT structure is still more than 10 million 49 kN wheel loads, which is long enough for normal roads in Japan.

Table 6 also presents the ratios of e_x and N_f to those of vehicle speed 5km/h and the material model V-0. When the vehicle speed is 5 km/h, e_x increases by 18 % from V-0 to V-2, which results in a 41 % less fatigue life. When the vehicle speed is 15 km/h, e_x increases by 8% from V-0 to V-2, which results in a 33 % less fatigue life. Therefore, not only viscosity of asphalt layer but also vehicle speed significantly affects fatigue life of asphalt layer.

Table 6. Tensile Strain at the Bottom of the Asphalt Layer Computed with 3DFEM and Fatigue Life.

	5km/h				10km/h				15km/h			
	e_x (10^{-6})		N_f		e_x (10^{-6})		N_f		e_x (10^{-6})		N_f	
V-0	86.8	1.00	2.38E+07	1.00	86.7	1.00	2.39E+07	1.00	85.9	0.99	2.47E+07	1.04
V-1	88.0	1.01	2.28E+07	0.96	87.6	1.01	2.32E+07	0.97	87.0	1.00	2.37E+07	0.99
V-2	102.1	1.18	1.40E+07	0.59	93.8	1.08	1.85E+07	0.78	92.8	1.07	1.91E+07	0.80

Conclusions

In this study, long term performance of HSCWT was investigated based on the results of repetitive loading tests in APT. Following remarks can be made:

- Stone and coin texture types on the bottom face of the panel effectively enhanced the bonding between the panel and grout.
- The sound bonding ensured very satisfactory long-term performance of HSC-WT.

Mechanical behavior of HSCWT under the travelling load was investigated with dynamic 3DEFM. Following remarks can be made:

- Although 3DFEM gave similar strain time histories to the measured ones, the visco-elastic properties of asphalt layer could not be clearly identified.
- Stresses in HSC panel is affected very little by visco-elastic parameters and loading rate. The most significant factor is the interface condition between the panel and grout.
- Stresses in the panel are much less than the strength of HSC panel if good bonding at the interface is provided. Therefore the fatigue of the panel would not be an issue in the structural design of HSC-WT.
- Fatigue life of asphalt layer estimated from tensile stress at the bottom of the asphalt layer is satisfactory for normal road in Japan.
- Not only viscosity of asphalt layer but also travelling speed significantly affects fatigue life of asphalt layer.

This study revealed that visco-elastic properties of asphalt layer significantly affect the fatigue life of HSCWT. More study is needed to clearly identify the visco-elastic properties of asphalt layer in HSCWT.

References

Japan Road Association (2007). *Pavement Design and Construction Guide*, Maruzen Co.

Huhtala, M. and J. Pilhajamaki (1992). "New Concepts on Load Equivalency Measurements." *Proceedings of 7th International Conference on Asphalt Pavements*, Vol. 3, 194-208.

Matsui, K. (1999). "*BALM 99: Back Analysis for Layer Moduli 1999 version*." The Japan FWD Users Group.

Nishizawa, T., et al (2005). "Dynamic Behavior of Ultrathin Whitetopping Structure with High Strength Concrete Under Traffic Load." *Proceedings of International Conference on Best Practice for ULTRATHIN and THIN Whitetoppings,* 151-175.

Nishizawa, T., Y. Murata, and K. Kokubu (2003). "Mechanical Behavior of Ultrathin Whitetopping Structure Under Stationary and Moving Loads." In *Transportation Research Record 1823*, pp. 102-110.

Sasaki, I., and T. Nishizaki (2004). "The Public Works Research Institute's Full-scale Pavement Investigations - Increasing Significance and Deployment of Reciprocating-type APT Facility." *Proceedings of 2nd International Conference on Accelerated Pavement Testing*.

Uzawa, M., T. Masuda, K. Shirai, Y. Shimoyama, and Y. Tanaka (2002). "Fresh Mortar Properties and Strength of Reactive Powder Composite Material." *Proceedings of 1st fib Congress 2002*, Session 7, 127-132.